Fifteenth USA/Europe Air Traffic Management Research and Development Seminar (ATM2023)

Strategic Planning of Aerial Assets for Disaster Response

Enabling Efficient and Equitable Access to Drone-Based Search Resources

Christopher Chin, Akila Saravanan, and Hamsa Balakrishnan
Department of Aeronautics and Astronautics
Massachusetts Institute of Technology
Cambridge, MA, USA
{chychin,akilasar,hamsa}@mit.edu

Adriana Andreeva-Mori
Aviation Technology Directorate
Japan Aerospace Exploration Agency
Tokyo, Japan
andreevamori.adriana@jaxa.jp

***Abstract*—The rapid deployment of fleets of small, uncrewed aircraft (drones) in the immediate aftermath of a natural disaster to search impacted regions for people in need of rescue is one of the most vital applications of advanced air mobility. Effective drone-based search operations require that the drone fleets operate out of bases that are appropriately located in advance of the disaster. Using a case study based in the Iwate prefecture of Japan, we develop optimization formulations to strategically locate drone bases. It is important to be capable of responding quickly to the locations most likely to require search, while covering as large an area as possible. We evaluate the disparities in the level of access afforded to different areas. Finally, we extend our optimization formulation to account for the probability of the base locations themselves being impacted by the disaster, and the possibility of base relocation.**

***Keywords*—applications of advanced air mobility; search and reconnaissance; large-scale disaster response;**

I. Introduction

The number of natural disasters experienced worldwide per decade have increased five-fold over the past 50 years, driven primarily by climate change and extreme weather [1]. Rising temperatures and warmer seas cause more water vapor to evaporate into the atmosphere, fueling storms like hurricanes, typhoons, and torrential rain. At the same time, urbanization and population growth have limited the area that can be used for water absorption after intense rains. Recent studies suggest that these factors compound and make floods the most common meteorological hazard, causing numerous casualties and significant property damage. In Japan, for example, approximately 41% of the population and 65% of national assets are concentrated in flood-prone areas [2], [3].

Large-scale natural disasters such as floods and earthquakes often disrupt ground infrastructure such as road networks [4], necessitating the use of alternative modes of sensing and transport for disaster response. Remote sensing with satellite imagery has played an important role in monitoring flood situations for risk and loss assessment [5]. However, clear images are rarely available in real-time due to operational constraints, tasking limitations of satellites, and occlusions such as clouds [6]. Consequently, aerial imaging—e.g., visual spotting of people needing to be rescued using conventional helicopters—plays a critical role in search operations immediately following a disaster event [7]. Advances in autonomy, the commercialization of small drones, and new imaging technologies have made drone-based aerial sensing a growing part of post-disaster search operations [8], [9]. Prior research has considered the tactical response during the search operation, such as the scheduling and routing of individual vehicles [10], [11]. An effective tactical response requires that the drones be staged in advance and flown from suitable base locations. Therefore, the *strategic* pre-disaster location of drone bases needs to be an integral part of disaster preparedness.

The objective of this work is to strategically choose base locations from where post-disaster search operations can be conducted using uncrewed aircraft (i.e., drones). The number of bases is constrained by the availability of trained personnel and aircraft, and the drones have limited flight times and range. It may not be possible to locate aerial assets (drone bases) so as to cover the entire region. Under such circumstances, it is important to strategically stage the bases in advance to be as responsive as possible to the areas most likely to need surveillance (e.g., because they are likely to have people in need of rescue). However, the choice of location can leave other regions far from a base, or possibly even without coverage. We therefore also evaluate the inequities in access to search resources that result from the choice of base locations. Finally, as the selected base location may itself be impacted by the disaster, we develop optimization formulations that account for uncertainty in base availability, as well as the possibility of relocating a base. We demonstrate our methods using a case study based on fleets of drones searching for evacuees who need to be rescued in the event of floods in the Iwate prefecture of Japan.

This research was supported in part by NSF CPS Award No. 1739505 and NASA University Leadership Initiative Grant #80NSSC20M0163, but this article solely reflects the opinions and conclusions of its authors and not NSF or any NASA entity. This research collaboration was also supported by the MIT Hayashi-ULVAC MISTI Seed Fund.

II. Related Work

As previously mentioned, there has been considerable work on the efficient distribution of tasks among drones, along with the optimization of their trajectories [11]–[13]. Optimization techniques such as dynamic vehicle routing [10], [14], [15] and neuro-fuzzy dynamic programming [16] have been proposed in this context. Large-scale optimization formulations have also been developed [17], [18]. Recent work has also focused on drone trajectory and mission assignment optimization [11]. Strategic disaster response planning [19] and base location problems [20] have similarities to those of aircraft base location [21], air ambulance base location planning [22], [23], set covering [24], and generalized facility location problems [25]. Equity of access, i.e., whether all regions or groups of people are being served in a fair manner, needs to be an important aspect of any public service, more so a life-saving one such as search-and-rescue. Transportation equity research has primarily focused on the potentially regressive impacts of pricing mechanisms [26]–[29]. However, with the growth of dynamic demand and on-demand services, the issue of equity in access to services has become a growing concern that needs to be addressed [30]. We draw from much of this literature in developing optimization formulations for strategically locating drone bases, taking into account the probability of search need and operational constraints. We evaluate the equity of access to bases by adapting the Gini coefficient, a metric traditionally used to measure income inequality [31], [32].

III. Problem Setup

We study the Iwate prefecture, which is the second largest prefecture in Japan, with an area of over 15,000 square kilometers. As of 2020, the Iwate prefecture ("Iwate") had a population of 1.2 million and had the lowest population density of any prefecture on Japan's main island, Honshu [33]. Fig. 1 shows the location and extent of Iwate. Many of its larger cities/towns lie in the Kitakami River valley, running vertically through the western half of Iwate. The coastal areas on the east also contain cities with more than 50,000 people, such as Kitakami and Miyako.

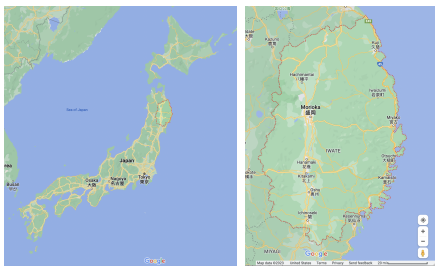

Figure 1: (Left) Map of Japan with Iwate prefecture shown within the red dotted line, and (Right) zoomed-in map of Iwate prefecture.

Like much of Japan, Iwate is susceptible to natural disasters, including earthquakes, tsunamis, and flooding. The March 2011 Tohoku earthquake, also referred to as the "Great East Japan Earthquake" was the most powerful earthquake recorded in Japan (and also the precursor to the infamous Fukushima accident) [34]. The coastal areas of Iwate were heavily impacted—tsunami waves triggered by the earthquake reached up to 40 meters (131 feet) in Iwate's coastal city of Miyako [35]. With over 15,000 deaths and $220 billion USD in damage, the Tohoku earthquake was the costliest natural disaster in world history [36]. As a rural prefecture susceptible to natural disasters, Iwate is conducive to deploying drones for disaster response. According to experts from JAXA and local government officials, drones would perform round-trip search and reconnaissance ("search") flights from pre-defined bases. The location of these bases will impact their effectiveness; bases located far away from areas requiring search would hamper operations. Locating bases as close as possible to potential search areas is not sufficient, as other objectives need to be considered. For example, before a disaster, the areas with search needs are uncertain, so it is important to locate bases such that they can cover large parts of the prefecture.

A. Input data

We divide Iwate into 15,452 1-km×1-km cells, denoted by the set I. We identified the set of candidate base locations J by consulting local experts. We assume that at most P number of bases can be opened. Since the range of drones deployed is uncertain, we assume that drones can search cells within a maximum distance L km of a base. At the time that base location decisions are made, we assume that for each cell i we have an estimated probability p_i that cell i will need to be searched. We estimate these probabilities based on four layers of spatial data: elevation, population, flooding locations, and rescue mission locations. As a disaster approaches, much more detailed data (e.g., real-time weather maps) could be used. But our formulations for base locations do not depend on how the search need probabilities are generated.

We used open-source elevation and population data. We defined the elevation of each cell as that of the centroid of each cell. We used the *Open Topo Data* API and the 30m SRTM database. A heat map of elevations in Iwate can be seen in Fig. 2a. The lighter pink colors correspond to areas of lower elevation. We used population data (obtained from the Iwate prefecture official website) for the 31 cities/towns in Iwate that are independent local government units. To identify areas of potential flooding, we used an existing JAXA hazard-risk area assessment. These largely correspond to the eastern coastal areas, as shown in Fig. 2c.

The rescue location data is based on scenarios generated by JAXA. One of the main challenges in disaster response planning is the limited availability of data. Because of privacy issues, information on the location and number of evacuees, for example, is only sporadically released. Data on rescue missions performed are typically only released in summary reports. JAXA's rescue mission database includes rescue locations and the number of evacuees at these locations. Data from past disasters, particularly the Great East Japan Earthquake and Tsunami, were used in the creation of the scenarios. JAXA also relied on interviews with local rescue authorities and input from subject-matter experts. Flight reports were obtained from local fire departments, medical assistance teams,

self-defense forces, police departments, and the coast guard. JAXA conducted interviews with pilots and rescue personnel involved in the relief mission to verify assumptions. The modeled rescue locations are shown in Fig. 2d.

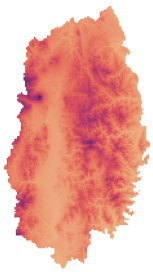

(a) Elevation (lighter colors indicate lower elevation).

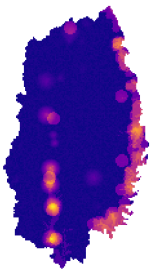

(b) Population (lighter colors indicate higher population).

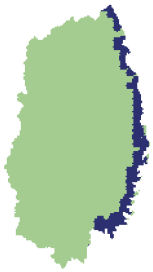

(c) Flooding areas (in blue)

(d) Rescue locations (in yellow).

Figure 2: Inputs used to estimate the probability of search need for each cell in Iwate prefecture.

B. Probabilities of needing search

Based on the input data layers, we then estimate the search need probability ("search probability") for each cell. This represents the probability that a cell will need to be searched during disaster response, i.e., that the cell might contain someone who needs to be rescued. We use the following procedure:

- **Initialization:** We initialize the probability of each cell using a uniform distribution in the range (0, 0.05).
- **Elevation:** We set 50 m (164 ft) as the elevation threshold. We increase the probability of the 603 cells with elevation less than this by 0.15.
- **Population:** We adjust cells based on nearby cities and towns. We set the city threshold as 8 km and the town threshold as 4 km. Cells within that threshold of a city/town had their probabilities increased by between (0, 0.25). For a given city/town we differentiate the probability increase of cells based on the distance from the city/town to the cell and the city/town population. Cells closest to large populations see the greatest increase in probability.
- **Prior flooding:** We set 3 km as the flooding threshold. Cells that lie within this threshold of a flooding location have their probability of search need increase by 0.25. This affects 1,413 cells.
- **Rescue:** We set 5 km as the rescue threshold. We increase the probability of the 1,976 cells within this threshold of a rescue location by 0.3.

Fig. 3 shows our estimated search probabilities. There is a high concentration of high-probability areas on the eastern coast. These low-elevation areas contain flooding and rescue locations. In the western half of Iwate, there is a vertical strip of higher probability area, which corresponds to the densely populated Kitakami River Valley in Iwate. The candidate base locations are indicated with squares. They are all independent local government units in Iwate Prefecture. Besides being more capable of supporting drone operations, these locations are typically used as ad hoc disaster response operations centers.

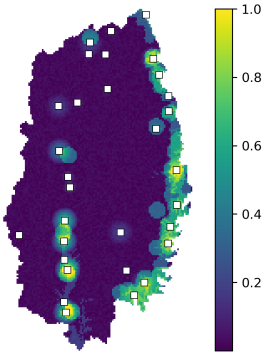

Figure 3: Estimated probabilities of search need, with candidate base locations indicated by white square icons.

IV. Optimizing Base Locations

A. Baseline Formulation

We first consider two priorities in base location: 1) maximizing coverage of the Iwate prefecture, and 2) minimizing the distance between bases and high-probability search areas. We use the following notation:

Sets

I: set of Iwate cells, indexed by i
J: set of candidate base locations, indexed by j

Parameters

p_i: probability of cell i needing search
d_{ij}: distance from cell i to base j
L: maximum distance between base and cell it serves
B_i: set of eligible bases within distance L of cell i
P: maximum number of bases

Decision Variables

$$x_j = \begin{cases} 1, & \text{if base } j \text{ is opened} \\ 0, & \text{otherwise} \end{cases}$$

$$z_i = \begin{cases} 1, & \text{if cell } i \text{ is covered} \\ 0, & \text{otherwise} \end{cases}$$

$$y_{ij} = \begin{cases} 1, & \text{if cell } i \text{ is covered and has closest base } j \\ 0, & \text{otherwise} \end{cases}$$

We consider a cell i to be "covered" if a base within distance L is open. Note that we also tested a formulation that considers base vehicle capacity constraints, but the base

locations generally did not change. The objective can be written as follows:

$$\max \ \alpha \sum_{i \in I} p_i z_i - \beta \sum_{i \in I} \sum_{j \in B_i} p_i d_{ij} y_{ij}$$

The first term of the objective rewards cells being covered by bases (we call this "coverage"). It is more rewarding to cover cells with a higher probability of search need. The second term minimizes the weighted distance between covered cells and their closest open base. The α and β coefficients indicate the trade-off between maximizing coverage and minimizing the distance to the nearest bases. As coverage increases, base locations will be more dispersed throughout Iwate, increasing the weighted distance between cells and open bases.

To simplify notation, we set $\alpha = 1$ and define $\gamma = \beta/\alpha$, as shown in expression (1). If $\gamma = 0$, the objective solely focuses on maximizing coverage. On the other hand, as γ goes to infinity, the second term of the objective dominates. This can lead to solutions where no bases are located with an objective value of 0. On an individual cell level, a cell i will not be covered if the distance penalty (second term of the objective) outweighs the coverage benefit (first term). In terms of variables, $z_i = 0$ if $\gamma > 1/d_{ij} \ \forall j \in B_i \cap \{j \in J | x_j = 1\}$. To avoid this issue, we specify $\gamma \leq 1/L$, since the maximum distance between a base and a cell it serves is L.

$$\max \ \sum_{i \in I} p_i z_i - \gamma \sum_{i \in I} \sum_{j \in B_i} p_i d_{ij} y_{ij} \tag{1}$$

$$s.t. \quad \sum_{j \in J} x_j \leq P \tag{2}$$

$$z_i \leq \sum_{j \in B_i} x_j \quad \forall i \in I \tag{3}$$

$$z_i \leq \sum_{j \in B_i} y_{ij} \quad \forall i \in I \tag{4}$$

$$y_{ij} \leq x_j \quad \forall i \in I, j \in B_i \tag{5}$$

$$\sum_{j \in B_i} y_{ij} \leq 1 \quad \forall i \in I \tag{6}$$

$$x_j, z_i, y_{ij} \in 0, 1 \quad \forall i, j \tag{7}$$

Constraint (2) sets the maximum number of bases to be located. Constraint (3) ensures that a cell is only counted as "covered" (denoted by z) if a base within L distance of it is opened (denoted by x). Constraint (4) relates z and y decision variables. If a cell is covered, then there exists at least one closest base (indicated by y). Constraint (5) helps define y_{ij}, which can only take a value of 1 if base j is opened. That is, a base j needs to be open for it to serve a cell i. Constraint (6) stipulates that each cell has at most one closest base.

We first evaluate the impact of P and L on base locations. We generated results for this paper with Gurobi on a 2019 MacbookPro with a 2.3 GHz 8-Core Intel Core i9 processor. Runtimes for the formulations ranged from 3–40 s (with the baseline formulation on the lower end and the formulation in Part IV-B on the higher end). We fix $\gamma = \frac{1}{5L}$ and vary P and L. Fig. 4 displays nine coverage maps for different P and L values. The yellow "X" marks indicate the chosen base locations. Cells that are colored light grey are "uncovered", meaning that their nearest base is more than L distance away. Cells that are colored the same share the same nearest base; for example, the orange points in Fig. 4a share the base in the western half of Iwate. The subfigure captions indicate the values of P and L used, and the coverage and mean distance to nearest base (DNB) is shown on top of each subfigure. As the number of bases or the radius L increases, more cells are covered. With $(P = 5, L = 50 \text{ km})$, 98.4% of cells are covered, compared to 39.3% with $(P = 3, L = 30 \text{ km})$. As P increases, the mean DNB generally decreases, as cells have more viable bases that can cover them. However, note that when coverage is low and a base is added to a region previously uncovered, then mean DNB can increase. For example, comparing $(P = 4, L = 30 \text{ km})$ and $(P = 5, L = 30 \text{ km})$, the 5th base (in orange) is added to a region almost entirely uncovered prior to the base being added. There are only a few cells between the blue and orange bases that see a reduction in DNB. Thus, we see that the mean DNB increases by 2.2%.

We next consider the impact of γ, which scales the distance term in the objective. Fig. 5 shows coverage metrics and distance metrics across different values of γ with $(P = 4, L = 40 \text{ km})$. We test $\gamma \in [0, 1/L]$: negative γ values would reward bases being far from cells, and $\gamma > 1/L$ would lead to cells not being covered (first term of objective) because of the penalty on the DNB of cells (second term of objective). The coverage proportion is defined as the percentage of cells that are covered. The weighted version includes the probability of each cell that is covered: $\sum_i p_i^{\text{covered}} / \sum_i p_i^{\text{all}}$. The mean distance to the nearest base metric is calculated across two sets: using only the covered cells, or using all of the cells (regardless of whether they are covered). The two Gini coefficients are calculated using the appropriate mean DNB values. We sort the array of DNB values in increasing order and calculate the Gini coefficient G as $\sum_{i=1}^{n} \frac{(2i-n-1)x_i}{n \sum_{i=1}^{n} x_i}$, where n is the number of data points. The Gini coefficient was first used to describe income inequality [31]. A Gini coefficient of 0 reflects perfect equality, whereas a value of 1 represents maximal inequality. Note that several values of γ result in identical base locations (and thus objective values). In Fig. 5, we connect values of γ with identical solutions with a line. Gaps between points indicate that the solution has changed. For example, $\gamma \in [0, 0.56]$ have the same base locations, but $\gamma = 0.56$ and $\gamma = 0.83$ correspond to different solutions. We did not evaluate the exact value of γ at which the solution changes, but we know its range: $(0.56, 0.83)$.

When $\gamma = 0$, the objective is solely to maximize coverage. As γ increases, the objective increasingly accounts for distances between covered cells and their nearest base. Thus, there is a trade-off between coverage and distances, which is shown by coverage decreasing as γ increases in the top panel of Fig. 5. The decrease in weighted coverage is less than that of unweighted coverage, indicating that the cells dropped from coverage tend to have lower p_i values. The mean DNB of covered cells decreases as γ increases since that is the term in the objective being scaled. But the mean DNB across all cells increases, as base locations are more

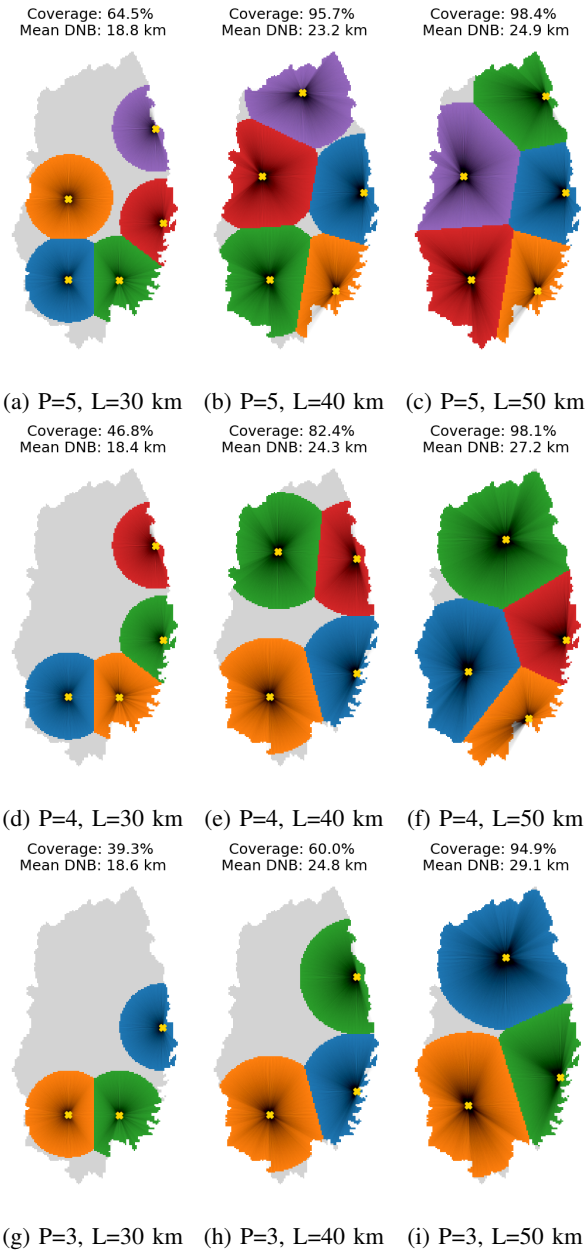

(a) P=5, L=30 km (b) P=5, L=40 km (c) P=5, L=50 km

(d) P=4, L=30 km (e) P=4, L=40 km (f) P=4, L=50 km

(g) P=3, L=30 km (h) P=3, L=40 km (i) P=3, L=50 km

Figure 4: Effect of varying the number of bases (P) and the maximum distance reachable from a base, L, when $\gamma = \frac{1}{5L}$. Coverage indicates the percentage of cells covered, and DNB stands for distance from a cell to the nearest base.

concentrated near high-probability search areas. In addition, the Gini coefficient for mean DNB among covered cells increases with γ. This means that the mean DNB distribution is becoming more unequal. Even though the mean DNB of covered cells decreases as γ increases, the Gini coefficient of covered cells actually increases. This indicates that some covered cells are receiving a disproportionate reduction in DNB.

We now examine some solutions described in Fig. 5 more closely. Fig. 6 shows coverage maps and DNB vs. probability of search need for three values of γ when $P = 4$ and $L = 40$ km. As γ increases, the left-hand side of the figure

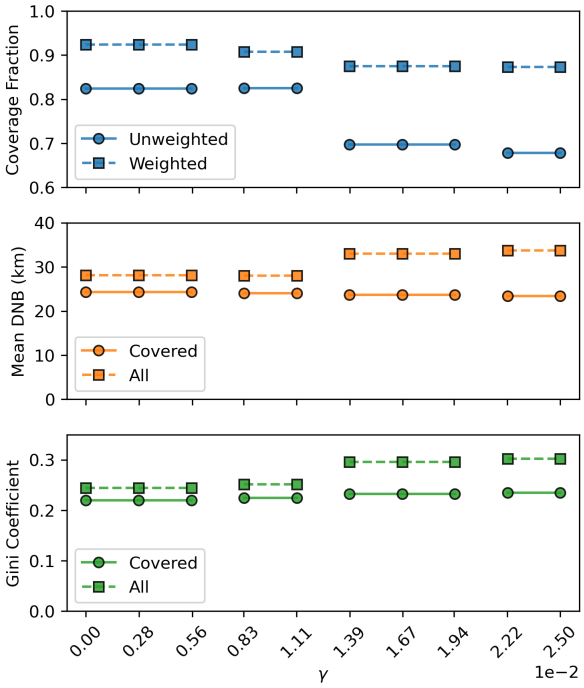

Figure 5: Coverage and distance metrics when varying γ. DNB stands for distance from a cell to the nearest base; Gini coefficient is calculated from DNB.

shows that bases shift toward the high probability cells on the coast and the southern spine (recall that the probabilities of search need are shown in Fig. 3). The right-hand side of the figure shows the distance to the nearest base as a function of the probability of a cell. Ideally, high-probability cells would be closer to their nearest base (i.e., we expect a negative relationship between the two). The red horizontal line indicates the value of L; points above the line are not covered, whereas points below are covered. As γ increases, cells with a high probability of search need benefit from a reduction in DNB. This comes at the expense of some lower probability cells that get bumped out of coverage. Specifically, with $\gamma = 0.56$e-2, the cells out of range tend to have lower probability; however, with $\gamma = 1.67$e-2, some cells with search probability between [0.5,0.75] are not covered. Overall, disaster response managers can use γ to trade-off between coverage and DNB. With increasing γ, although DNB among covered cells decreases, inequality (either with respect to all cells or covered cells) decreases, as the base locations tilt toward high-probability cells.

B. Uncertainty in base availability

Up to this point, we have assumed that the chosen base locations will be operable immediately following a disaster. This may not always be the case, as some of the base locations may be impacted by earthquakes or flooding. When this occurs, other bases may need to cover a cell, even if they were previously not the closest base. Thus, it may be desirable to have multiple bases able to cover a given cell. We adopt the maximum expected covering location model, which

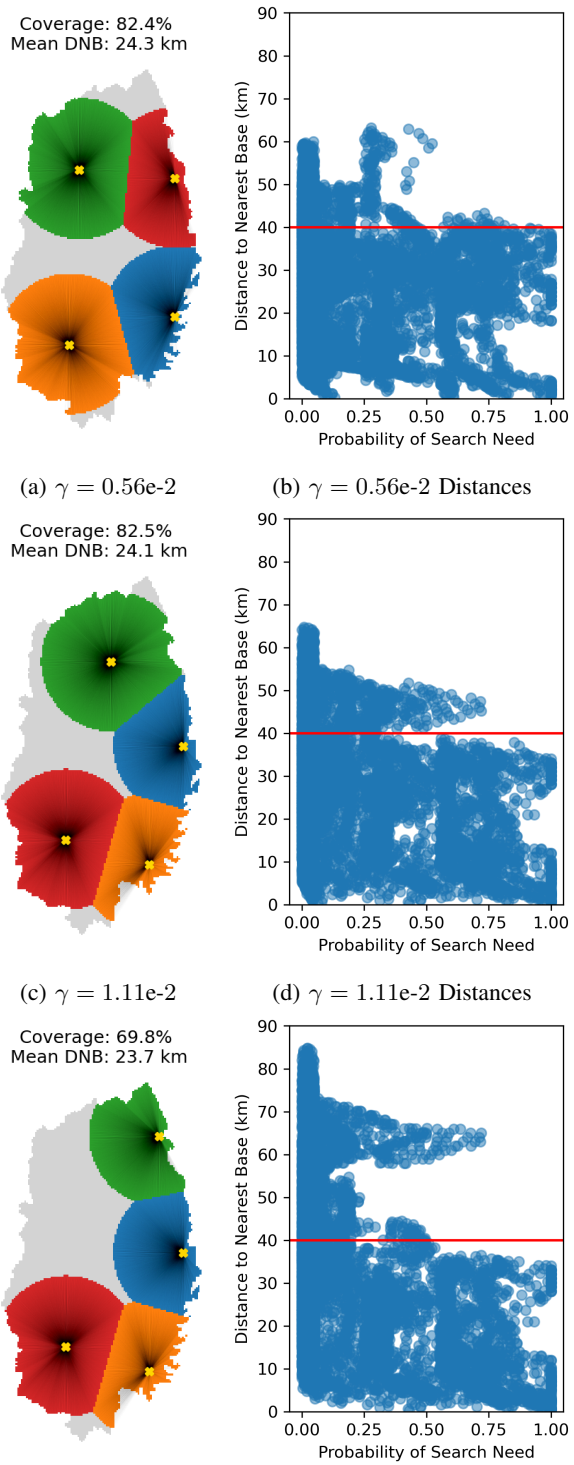

(a) $\gamma = 0.56$e-2 (b) $\gamma = 0.56$e-2 Distances

(c) $\gamma = 1.11$e-2 (d) $\gamma = 1.11$e-2 Distances

(e) $\gamma = 1.67$e-2 (f) $\gamma = 1.67$e-2 Distances

Figure 6: Impact of γ on Distance to Nearest Base (DNB) and coverage; $P = 4, L = 40$ km.

acknowledges that not all bases are guaranteed to be operable [24]. We assume that bases are inoperable with independent yet identical probability $r \in [0, 1)$. These assumptions reduce complexity and allow the number of operating bases to follow a binomial distribution. The binomial distribution enables the following statements.

- Prob(cell i is covered by a working base, given there are k bases that can serve it) $= 1 - r^k$
- P_{ik}: random variable representing "reward" at cell i given that k bases can serve i. We use p_i (the probability of search need) as the reward, and this occurs with probability $1 - r^k$
- The expectation of P_{ik} is $E(P_{ik}) = p_i(1 - r^k)$
- $\Delta E(P_{ik}) = E(P_{i,k}) - E(P_{i,k-1}) = p_i(1-r)r^{k-1}$ when increasing number of bases that can cover cell i from $k - 1$ to k.

We can now incorporate the likelihood of base failure into the objective. We define the following additional decision variable.

$$v_{ik} = \begin{cases} 1, & \text{if there are } k \text{ bases that could serve cell } i \\ 0, & \text{otherwise} \end{cases}$$

When we locate bases, we control v_{ik} as we have P bases and we know the maximum distance L between a base and a cell that it covers. Therefore, in the objective, we want to reward locating more bases that could serve a cell. The incremental benefit in locating an additional base close enough to cover a cell is given by $\Delta E(P_{ik})$. Thus, we can write the objectives as follows. The objective follows the same form as (1), with the second distance-related term being identical. The difference is in the scaling of the coverage term (the first term).

$$\max \ \alpha \sum_{i \in I} \sum_{k=1}^{P} (1-r) r^{k-1} v_{ik} p_i z_i - \beta \sum_{i \in I} \sum_{j \in B_i} p_i d_{ij} y_{ij} \tag{8}$$

$$s.t. \quad (2) - (7)$$

$$\sum_{k=1}^{P} v_{ik} \leq \sum_{j \in B_i} x_j \quad \forall i \in I \tag{9}$$

$$y_{ij} \in 0, 1 \quad \forall i, j \tag{10}$$

Constraint (9) relates v_{ik} to the locating of bases (x_j). The left-hand side of the constraint represents the total number of bases that can cover cell i. This must not exceed the number of *located* bases that can serve i. Note that we do not explicitly encode an ordering constraint of v_{ik} variables for a given i and $k = 1, 2, 3, \ldots$. This is because the maximization objective ensures that if $\sum_{k=1}^{P} v_{ik} = 1$, then $v_{i1} = 1$ and $v_{i2} = 0$. (The reward for locating the first base close enough to cover a cell is larger than the reward for locating a second base.) Unlike γ, which is capped at $1/L$, we do not set a maximum value of r. With large γ values, not covering some individual cells was more rewarding than covering them—this is not an issue here. As r increases, the first term of the objective will dominate, and the DNB metric is de-emphasized.

Fig. 7 follows the layout of Fig. 5, but varies r instead of γ, and Fig. 8 displays the coverage map and DNB vs. probability of search need plots for $r \in \{0.3, 0.6\}$, as well as the coverage maps for $r \in \{0.7, 0.8, 0.9\}$. The value of γ was fixed at 1.67e-2. The points for $r \in \{0.3, 0.4, 0.5\}$ are connected because they result in the same base locations. When comparing Fig. 8 to Fig. 6, we see that large values

of r result in more clustering than with large values of γ. Fig. 8d shows that for $r = 0.6$ the *covered* cells with a high search probability tend to have lower DNB. However, there are many cells with a high search probability that are left uncovered, particularly when compared to $r = 0.3$ (Fig. 8b).

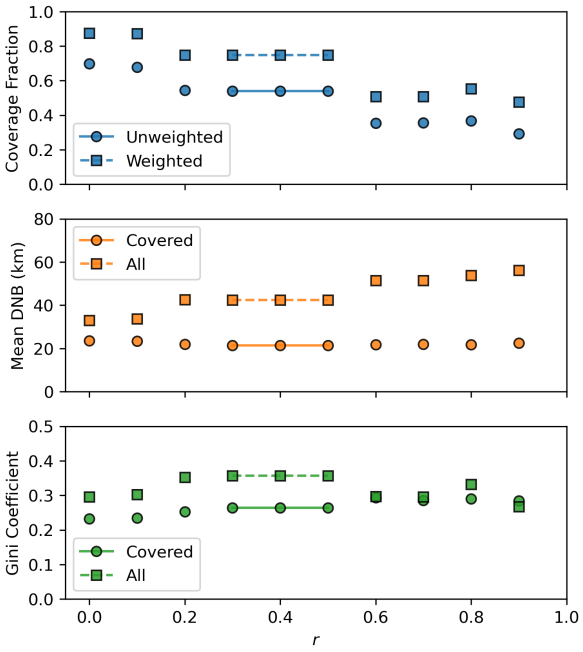

Figure 7: Coverage and distance metrics when varying r. DNB stands for distance from a cell to the nearest base; Gini coefficient is calculated from DNB.

As r increases (i.e., bases are more likely to become inoperable), the weighted and unweighted cell coverage generally decreases. The exception is $r = 0.8$, where the inland location in Fig. 8f increases coverage relative to $r = 0.7$ (Fig. 8e). In general, the mean DNB of covered cells decreases, whereas the mean DNB across all cells increases. The Gini coefficient also tends to increase with r, but has some nuances. Notably, $r = 0.7$ and $r = 0.9$ have lower Gini coefficients than $r = 0.8$ because of their clustering of base locations. The low Gini coefficient across all cells could be misleading for $r = 0.9$, as the base locations (Fig. 8g) on the eastern coast cause many uncovered cells to be "equally bad off" based on their far distance to the nearest base.

V. Relocation of Bases

In Section IV-B, we considered the possibility that bases may become inoperable during disaster response. The formulation we presented handles this by building in redundancy such that it is preferable to open multiple bases capable of covering cells. However, in practice, it may be possible to relocate bases (i.e., close a base in location j and open a base in location k). This may occur when base j becomes inoperable, or when the probabilities of search need change drastically relative to the probabilities that dictated the initial base allocation. We first present a model to optimally relocate bases in Section V-A, before incorporating the possibility of relocation in the initial base allocation in Section V-B.

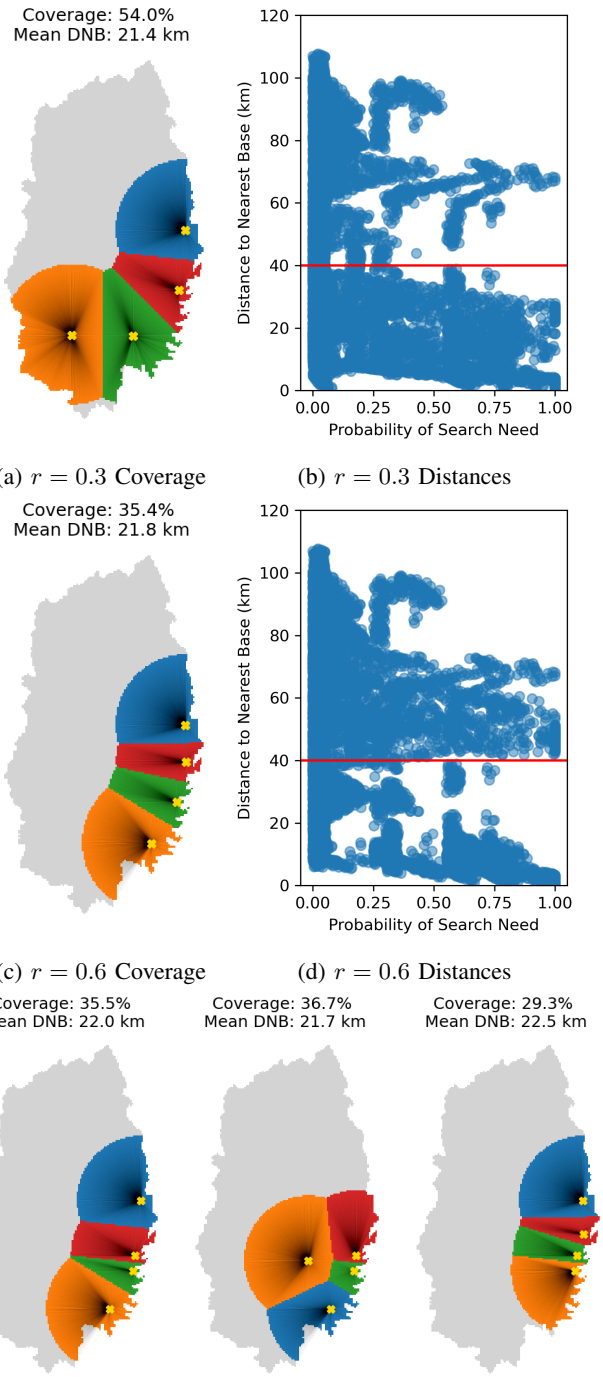

(a) $r = 0.3$ Coverage (b) $r = 0.3$ Distances

(c) $r = 0.6$ Coverage (d) $r = 0.6$ Distances

(e) $r = 0.7$ Coverage (f) $r = 0.8$ Coverage (g) $r = 0.9$ Coverage

Figure 8: Impact of varying probability of base unavailability, r. $P = 4, L = 40$ km.

A. Base Relocation Formulation

Suppose that we now have the flexibility to relocate up to R bases after initial base allocation. The maximum distance that a base can be moved is D. We introduce the following additional sets, parameters, and variables while keeping the same notation from Section IV.

Sets & Parameters

J_1: set of existing base locations
J_2: set of new potential base locations
J: set of all base locations, equal to $J_1 \cup J_2$
K_j set of locations that base j could relocate to
R_k: set of bases that could relocate to k
R: maximum number of bases that can be relocated
D: maximum distance that a base can be moved ("relocation radius")

Decision Variables

$m_{jk} = 1$ if base j is closed and base k is opened ("relocation" from j to k); 0 otherwise
v_{jk}: binary variable for big-M notation

The relocation radius D is used to define K_j, the list of eligible relocation sites for each existing base. Note the distinction between K_j and R_k: the former indicates locations that j could move *to*; the latter represents locations that k could move *from*. We still use the x decision variable to denote locating bases, with reference to the appropriate set of J_1 or J_2. If $x_j = 1$ and $j \in J1$, then an existing base location remains open. On the other hand, if $j \in J2$, then a base was relocated. The objective function remains the same as expression (1). We introduce several new constraints.

$$\max \sum_{i \in I} p_i z_i - \gamma \sum_{i \in I} \sum_{j \in B_i} p_i d_{ij} y_{ij}$$

$$s.t. \quad (2) - (7)$$

$$m_{jk} \leq M v_{jk} \quad \forall j \in J_1, k \in K_j \tag{11}$$

$$x_j \leq M(1 - \sum_{k \in K_j} v_{jk}) \quad \forall j \in J_1 \tag{12}$$

$$x_k \leq m_{jk} \quad \forall j \in J_1, k \in K_j \tag{13}$$

$$\sum_{j \in R_k} m_{jk} \leq 1 \quad \forall k \in J_2 \tag{14}$$

$$\sum_{k \in K_j} m_{jk} \leq 1 \quad \forall j \in J_1 \tag{15}$$

$$\sum_{j \in J_1} \sum_{k \in K_j} m_{jk} \leq R \tag{16}$$

$$m_{jk}, v_{jk} \in 0, 1 \quad \forall j, k \tag{17}$$

Constraint (11) and (12) use Big-M notation to establish the dependence between m_{jk} and x_j for existing base locations. Specifically, if $m_{jk} = 1$, then constraint (11) requires that $v_{jk} = 1$. From constraint (12), this requires that $x_j = 0$. In words, this means that for a base to move from j to k, base j must close. In addition, if $x_j = 1$ (i.e., base j remains open), then $v_{jk} = 0 \ \forall j \in J_1, k \in K_j$. This means that $m_{jk} = 0$, so no base can be opened as a result of moving base j. Constraint (13) relates m_{jk} to x_k for the new potential base locations. In order for base k to open, m_{jk} must equal 1, meaning that base j was closed. Constraint (14) indicates that a new base $k \in J_2$ can only be opened once, while Constraint (15) means that an existing base $j \in J_1$ can only be relocated once. Constraint (16) limits the number of base relocations to R.

B. Planning for Potential Relocation (PPR) Formulation

With limits on the number of bases that can be relocated and the maximum distance that a base can be relocated, the effectiveness of base location depends on the initial base allocation. Thus, we now consider planning for potential relocation in the initial allocation. We call this the PPR (planning for potential relocation) formulation. We define the following additional decision variables.

$$w_k = \begin{cases} 1, & \text{if base } k \text{ could be relocated to} \\ 0, & \text{otherwise} \end{cases}$$

$$u_i = \begin{cases} 1, & \text{if cell } i \text{ is covered by potential relocation site} \\ 0, & \text{otherwise} \end{cases}$$

We augment the objective function of 1, whose first term rewards coverage of a cell with the initial base allocation. The additional term rewards being able to *relocate* to a base that can cover a cell. We set $\lambda < 1$ so that covering a cell now is more rewarding than potentially covering it with future base relocation. The decision variable u_i is analogous to z_i in that it rewards coverage of cells.

$$\max \sum_{i \in I} p_i z_i - \gamma \sum_{i \in I} \sum_{j \in B_i} p_i d_{ij} y_{ij} + \lambda \sum_{i \in I} p_i u_i$$

$$s.t. \quad (2) - (7)$$

$$w_k \leq \sum_{j \in R_k} x_j \quad \forall k \in J \tag{18}$$

$$u_i \leq \sum_{k \in B_i} w_k \quad \forall i \in I \tag{19}$$

$$w_j \leq 1 - x_j \quad \forall j \in J \tag{20}$$

$$u_i, w_j \in 0, 1 \quad \forall i, j \tag{21}$$

The variable w_k indicates whether a base—not initially opened—could be relocated *to* in the future, given the relocation radius constraint. Constraint 18 requires that a base close enough to k is opened for w_k to equal 1. Constraint 19 relates the coverage indicator u_i if cell i could be served a future base relocation. Constraint 20 ensures that an open base is not counted as a candidate for relocation.

C. Experimental Results

We now compare the PPR formulation with the baseline formulation. We fix several parameters, including $P = 5$, $L = 30$ km, $\gamma = \frac{1}{2L}$. Specific to relocation, we set $\lambda = 0.5$ and allow 2 bases to be moved ($R = 2$) up to 30 km ($D = 30$). We first perform the initial base allocation using the same search probabilities that we have been using. Next, we randomly generate a new set of search probabilities. We do not alter the input layers of Section III.A but randomly set the relative weight given to each of the four layers (elevation, population, flooding, and rescue). For example, previously we increased the search probability need of low-elevation cells by 0.15; here, we still increase the probability of all low-elevation cells by the same amount, but not necessarily by 0.15. We set the relative weight of each of the four layers while making sure that no cell has search probability greater than 1. Once the updated search probabilities are generated, we relocate bases based on the formulation in Section V-A.

Fig. 9a shows the initial search probabilities, while Fig. 9b displays the updated search probabilities. Because of our

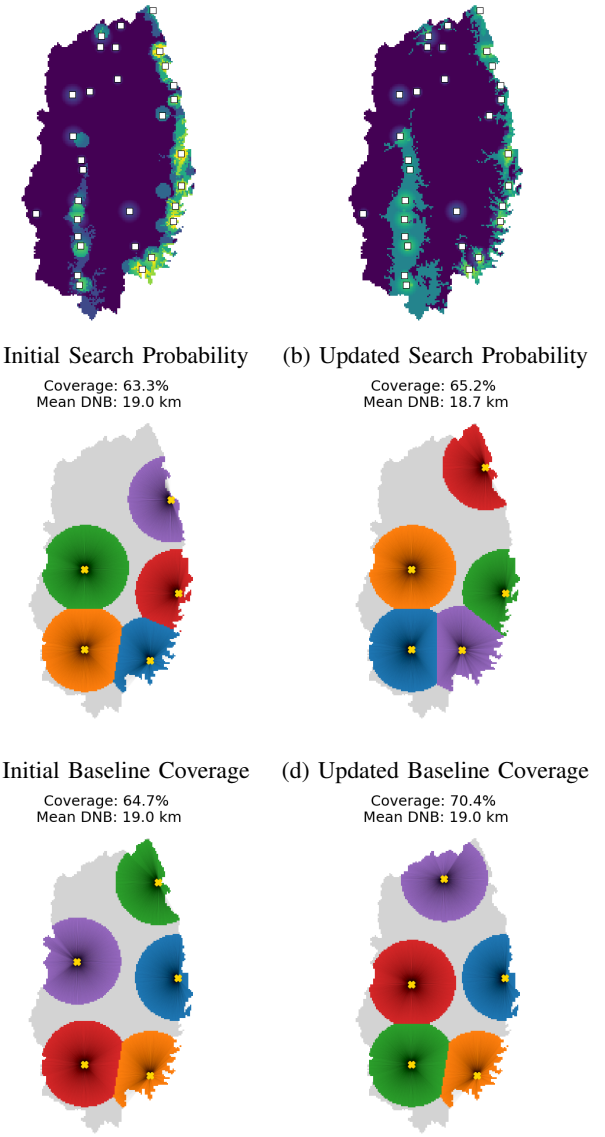

(a) Initial Search Probability (b) Updated Search Probability

(c) Initial Baseline Coverage (d) Updated Baseline Coverage

(e) Initial PPR Coverage (f) Updated PPR Coverage

Figure 9: Baseline vs. PPR (Planning for Potential Relocation) Formulation when $\gamma = \frac{1}{2L}$, $P = 5$, $L = 30$ km, $\lambda = 0.5$. Left-column shows the pre-relocation setting; right-column shows the post-relocation setting.

probability generation process, the updated search probability looks somewhat similar to the initial search probability. This is intentional, as we assume that our initial search probabilities will not be completely incorrect. The second row of Fig. 9 shows the initial and updated coverage maps using the baseline formulation, and the third row shows the same for the PPR formulation. We note that the PPR formulation spaces bases further apart to allow for more base relocation options. This conservatism benefits the PPR formulation in Fig. 9f, as the purple base in northern tip of Iwate is relocated to, corresponding with a high probability cluster.

We perform 100 trials with randomly generated initial and updated search probabilities. The other parameters (e.g., number of bases, relocation radius) remain the same as Fig. 9. Table I compares the performance of the PPR and baseline formulations after base relocation. The numbers indicate the mean percent difference between PPR and Baseline for six metrics. Pre-relocation, the PPR formulation on average has 2.3% more unweighted cell coverage, but 4.1% less weighted coverage. In addition, the PPR formulation has worse mean DNB and Gini coefficient metrics among covered cells, but better among all cells. We now consider the post-relocation metrics. The PPR formulation results in 8.1% higher unweighted coverage on average than the baseline formulation. The PPR formulation also has a 4.1% higher mean weighted cell coverage. The mean DNB among covered cells is similar between PPR and baseline, with PPR having slightly higher values on average. However, the PPR formulation has a large advantage in mean DNB among all cells. We also see lower Gini Coefficient values for the PPR formulation. Overall, the PPR formulation has a clear advantage in coverage, distance, and Gini coefficient metrics post-relocation. However, the trade-off comes pre-relocation where the baseline formulation generally has better metrics among *covered* cells, but not among all cells. If the search probabilities do not drastically change, base relocation may not be needed. In this paper, we did not test the ability to relocate bases even when the search probabilities remain the same.

TABLE I. PERCENT DIFFERENCE BETWEEN PPR AND BASELINE FORMULATIONS. POSITIVE NUMBERS INDICATE HIGHER VALUES FOR THE PPR FORMULATION

Metric	Type	Pre-relocation Metrics	Post-relocation Metrics
Cell Coverage	Unweighted	2.3	8.1
	Weighted	-4.1	4.3
Mean Distance to Nearest Base	Covered	2.7	0.3
	All	-9.5	-8.2
Gini Coefficient	Covered	1.9	-1.3
	All	-13.1	-12.3

VI. CONCLUSIONS

In the immediate aftermath of a disaster, it is important to quickly perform search and reconnaissance, followed by rescue operations. In this paper, we focused on strategic base location as it significantly influences the effectiveness of drone operations, through a case study of the Iwate prefecture in Japan. We first generated search need probabilities and then tested a baseline formulation that tried to: (1) maximize coverage, and (2) minimize the distance between covered cells and their nearest base (DNB). We also considered Gini coefficient metrics based on the DNB values. We showed the impact of the γ parameter, which controls the trade-off between coverage and DNB values. We also adopted a maximum covering formulation to account for uncertainty in base availability.Building in this redundancy led to clustering of base locations, but a reduction in coverage, a worsening of DNB metrics, and poorer Gini coefficients. We then presented a formulation which allowed for the relocation of a limited number of bases, and a formulation that prepared for the possibility of relocation from the start (the PPR formulation). We found that the PPR formulation outperformed the baseline

formulation in the event of base relocation, but was slightly worse pre-relocation.

Future work will incorporate tactical aspects of the disaster response, such as task assignment and vehicle routing. Doing so will allow us to evaluate metrics based on reconnaissance time. There is also opportunity to relax some of the simplifying assumptions made in this work (e.g., the independence of base availability), and to develop real-time base relocation support for decision-makers. Finally, since the goal of search is to inform rescue operations, the coordination of drones (for search) and crewed aircraft (for rescue) is an important practical aspect that needs to be addressed.

REFERENCES

[1] World Meteorological Organization (WMO), "Weather-related disasters increase over past 50 years, causing more damage but fewer deaths," 2011. [Online]. Available: https://public.wmo.int/en/media/press-release/weather-related-disasters-increase-over-past-50-years-causing-more-damage-fewer

[2] Z. W. Kundzewicz, S. Kanae, S. I. Seneviratne, J. Handmer, N. Nicholls, P. Peduzzi, R. Mechler, L. M. Bouwer, N. Arnell, K. Mach, R. Muir-Wood, G. R. Brakenridge, W. Kron, G. Benito, Y. Honda, K. Takahashi, and B. Sherstyukov, "Flood risk and climate change: global and regional perspectives," *Hydrological Sciences Journal*, vol. 59, no. 1, 2014.

[3] Institute for Water Resources (IWR), US Army Corps of Engineers), "Flood risk management approaches: as being practiced in Japan, Netherlands, United Kingdom and United States," 2011.

[4] A. A. Ganin, E. Massaro, A. Gutfraind, N. Steen, J. M. Keisler, A. Kott, R. Mangoubi, and I. Linkov, "Operational resilience: concepts, design and analysis," *Scientific reports*, vol. 6, 2016.

[5] J. Gomi, "Supporting disaster management with space applications," http://global.jaxa.jp/article/special/antidisaster/gomi_e.html.

[6] E. Robinson, H. Balakrishnan, M. Abramson, and S. Kolitz, "Optimized stochastic coordinated planning of asynchronous air and space assets," *AIAA Journal of Aerospace Information Systems*, vol. 14, no. 1, pp. 10–25, 2017.

[7] A. Andreeva-Mori, K. Kobayashi, and M. Shindo, "Particle swarm optimization/greedy-search algorithm for helicopter mission assignment in disaster relief," *Journal of Aerospace Information Systems*, vol. 12, no. 10, pp. 646–660, 2015.

[8] S. Chowdhury, A. Emelogu, M. Marufuzzaman, S. G. Nurre, and L. Bian, "Drones for disaster response and relief operations: A continuous approximation model," *International Journal of Production Economics*, vol. 188, pp. 167–184, 2017.

[9] R. R. Murphy, *Disaster Robotics (Intelligent Robotics and Autonomous Agents series)*. The MIT Press, 2014.

[10] C.-F. Hsueh, H.-K. Chen, and H.-W. Chou, "Dynamic vehicle routing for relief logistics in natural disasters," in *Vehicle Routing Problem*, T. Caric and H. Gold, Eds. Rijeka: IntechOpen, 2008, ch. 5. [Online]. Available: https://doi.org/10.5772/5641

[11] A. Andreeva-Mori, J. Homola, M. Johnson, K. Kobayashi, Y. Okuno, and P. Kopardekar, "Integrated UAS trajectory optimization for disaster response reconnaissance missions," in *ICAS*, 2022.

[12] A. Balasingam, K. Gopalakrishnan, R. Mittal, M. Alizadeh, H. Balakrishnan, and H. Balakrishnan, "Toward a marketplace for aerial computing," in *DroNet 2021 – 7th ACM Workshop on Micro Aerial Vehicle Networks, Systems, and Applications*, 2021.

[13] C. Chin, K. Gopalakrishnan, M. Egorov, A. Evans, and H. Balakrishnan, "Efficiency and fairness in unmanned air traffic flow management," *IEEE Trans. on Intelligent Transportation Systems*, vol. 20, no. 9, 2021.

[14] N. Roy, W. Burgard, D. Fox, and S. Thrun, "Coastal navigation-mobile robot navigation with uncertainty in dynamic environments," in *Proceedings 1999 IEEE International Conference on Robotics and Automation (ICRA)*, 1999.

[15] A. Balasingam, K. Gopalakrishnan, R. Mittal, V. Arun, A. Saeed, M. Alizadeh, H. Balakrishnan, and H. Balakrishnan, "Throughput-fairness tradeoffs in mobility platforms," in *ACM MobiSys 2021*, 2021.

[16] N. Hanlon, M. Kumar, and K. Cohen, "Neuro-fuzzy dynamic programming for decision-making and resource allocation during wildland fires," in *51st AIAA Aerospace Sciences Meeting Proceedings*, 2013.

[17] H. Balakrishnan and B. Chandran, "A distributed framework for traffic flow management in the presence of unmanned aircraft," in *Proceedings of the USA/Europe Air Traffic Management R&D Seminar*, 2017.

[18] L. Ozdamar, "Planning helicopter logistics in disaster relief," *OR Spectrum*, vol. 33, 2011.

[19] C. Boonmee, M. Arimura, and T. Asada, "Facility location optimization model for emergency humanitarian logistics," *International Journal of Disaster Risk Reduction*, vol. 24, pp. 485–498, 2017.

[20] A. Verma and G. M. Gaukler, "Pre-positioning disaster response facilities at safe locations: An evaluation of deterministic and stochastic modeling approaches," *Computers & Operations Research*, vol. 62, pp. 197–209, 2015.

[21] R. Gopalan, "The aircraft maintenance base location problem," *European Journal of Operational Research*, vol. 236, no. 2, pp. 634–642, 2014.

[22] C. J. Jagtenberg, M. A. Vollebergh, O. Uleberg, and J. Røislien, "Introducing fairness in Norwegian air ambulance base location planning," *Scandinavian Journal of Trauma, Resuscitation and Emergency Medicine*, vol. 29, 2021.

[23] B. Villarreal, E. A. Granda-Gutierrez, S. Lankenau, A. C. Bastidas, and A. Montalvo, "Decreasing ambulance response time through an optimal base location," in *Proceedings of the 2017 international symposium on industrial engineering and operations management (IEOM)*, 2017.

[24] M. S. Daskin, "A maximum expected covering location model: Formulation, properties and heuristic solution," *Transportation Science*, vol. 17, no. 1, pp. 48–70, 1983. [Online]. Available: https://doi.org/10.1287/trsc.17.1.48

[25] Q. Wang, R. Batta, J. Bhadury, and C. M. Rump, "Budget constrained location problem with opening and closing of facilities," *Computers Operations Research*, vol. 30, no. 13, pp. 2047–2069, 2003. [Online]. Available: https://www.sciencedirect.com/science/article/pii/S0305054802001235

[26] F. Ramjerdi, "Equity measures and their performances in transport," *Transportation Research Record*, 2006. [Online]. Available: 10.1177/0361198106198300110

[27] T. Langmyhr, "Managing equity: The case of road pricing," *Transport Policy*, vol. 4, no. 1, pp. 25–39, 1997.

[28] P. Decorla-Souza, "Income-Based Equity Impacts of Congestion Pricing," *Federal Highway administration*, 2008.

[29] J. Eliasson, "Is congestion pricing fair?" *Transport Policy*, vol. 52, pp. 1–15, 2016.

[30] S. R. Middleton, "Discrimination, Regulation, and Design in Ridehailing," Massachusetts Institute of Technology SM Thesis, 2018.

[31] C. Gini, "Measurement of inequality of incomes," *The Economic Journal*, vol. 31, no. 121, pp. 124–126, 1921. [Online]. Available: http://www.jstor.org/stable/2223319

[32] T. Drezner, Z. Drezner, and J. Guyse, "Equitable service by a facility: Minimizing the gini coefficient," *Computers Operations Research*, vol. 36, no. 12, pp. 3240–3246, 2009.

[33] Statistics Bureau of Japan, "2020 population census," May 2022.

[34] Y. Wakatsuki and K. Lah, "3 nuclear reactors melted down after quake, japan confirms," Jun 2011. [Online]. Available: http://www.cnn.com/2011/WORLD/asiapcf/06/06/japan-nuclear.meltdown/index.html

[35] Y. Tsuji, K. Satake, T. Ishibe, T. Harada, A. Nishiyama, and S. Kusumoto, "Tsunami heights along the pacific coast of northern honshu recorded from the 2011 tohoku and previous great earthquakes," *Pure and Applied Geophysics*, vol. 171, no. 12, p. 3183–3215, 2014.

[36] "Japan damage could reach $235 billion, world bank estimates," Mar 2011. [Online]. Available: https://latimes.com/business/la-fgw-japan-quake-world-bank-20110322,0,3799976.story

AUTHOR BIOGRAPHIES

Christopher Chin is a PhD Candidate in the Department of Aeronautics and Astronautics at the Massachusetts Institute of Technology (MIT).

Akila Saravanan is an undergraduate student majoring in Aeronautics & Astronautics, and Electrical Engineering & Computer Science at MIT.

Hamsa Balakrishnan is the William E. Leonhard (1940) Professor of Aeronautics and Astronautics at MIT.

Adriana Andreeva-Mori is an associate senior researcher in the Aviation Technology Directorate at the Japanese Aerospace Exploration Agency (JAXA).